

Thermodynamic Parameters and Influence of Kinetic Factors on the Self-Assembly of Acid-Soluble Collagen Nanofibrils

Fatemeh Elmi¹ · Maryam Mitra Elmi² · Fatemeh Nasiri Amiri¹

Received: 12 March 2017 / Accepted: 12 June 2017 / Published online: 8 July 2017
© Springer Science+Business Media, LLC 2017

Abstract In this study, the acid-soluble collagen (ASC), extracted from the fish scales of the Caspian white fish (*Rutilus Firisikutum*) was studied. The thermo-gravimetric analysis (TGA) showed the maximum demineralization accomplished after 48 h of EDTA treatment. SDS-PAGE and FT-IR spectroscopy confirmed that extracted ASC was mainly type I collagen. FE-SEM images confirmed the porous and filamentary structure. The denaturation temperature (T_d) of ASC was 19 °C, and the transition heat achieved 9.6 J/g. Collagen self-assembly exhibit important potential because for biomedical applications and green technologies. Various inter- and intramolecular no-covalent interactions such as hydrogen bonding, hydrophobic, electrostatic and Van der Waals interactions influence the formation of self-assembled collagen. Therefore, critical factors as concentration of ASC, temperature, pH, and ionic strength play crucial role in function integration and structural modulation. The impacts of those external triggers on the kinetic self-assembly of ASC demonstrated a two-phase kinetic process, a sigmoidal plot. ACS showed pronounced self-assembly behavior when temperature and

concentration reach above 14 °C and 0.125 mg/ml, higher concentration and/or temperature could stimulate the ASC self-assembly. The optimum pH value for ASC self-assembly was pH = 7. The effect of ionic strength on ASC self-assembly showed the turbidity increases significantly in 131.2 mM salt concentration. The process of self-assembly is mainly driven by thermodynamics. The thermodynamic study of collagen self-assembly illustrated that the activation energy, $E_a = 44.3$ kJ/mol, the frequency factor, $A = 117 \times 10^5$ s⁻¹, the enthalpy transition, $\Delta H^\ddagger = 42.98$ kJ/mol, and the entropy transition, $\Delta S^\ddagger = -0.12$ kJ/mol.K, respectively. These findings show that kinetics factors not only influence the self-assembly structure of ASC but also regulate the activation complex structure in the transition state.

Keywords Collagen · Fish Scale · Nano Fibril · Self-Assembly · Kinetics · Thermodynamic

Introduction

Collagen is a fibrous protein in connective tissues, widely used for biomedical and pharmaceutical purposes. Type I collagen is the main protein of the extracellular matrix (ECM), which can play a critical role in the mechanical protection of tissues [1]. The self-assembling trait of collagen plays a crucial role in its physiological functions, and has attracted increasing attention due to its great potential for biological and industrial applications. In vivo, the presence of a variety of enzymes, especially for those cross-linking the collagen and other components of ECM, can promote the self-assembly of collagen, which has natural advantages for the regeneration of tissues. However, both in vivo and in vitro, type I collagen

Electronic supplementary material The online version of this article (doi:10.1007/s11483-017-9492-5) contains supplementary material, which is available to authorized users.

✉ Fatemeh Elmi
f.elmi@umz.ac.ir

¹ Department of Marine Chemistry, Faculty of Marine & oceanic sciences, University of Mazandaran, Babolsar, Iran

² Cellular and Molecular Biology Research Center, Health Research Institute, Babol University of Medical Sciences, Babol, Iran

triple monomers self-assemble into fibrillar structures, which may entangle and/or cross-link to form visco-elastic gels with widely different mechanical properties and network structures [2]. Therefore, switching between different configurations through external triggers will even gain the construction of smart hierarchical fibrillar structures.

Kinetic self-assembly processes are fundamental for understanding the nature of collagen self-assembly. The characterization techniques such as TEM, are more structurally aimed and have rarely been applied to visualize the developing networks or cross linkages [3–5]. The dominant method to study self-assembly is turbidity [6]. The turbidometric curve contains two phases, a lag phase with no measurable change in turbidity and a growth phase by a sigmoidal change. Some variables such as temperature, concentration, pH, and ionic strength can affect the kinetics of collagen self-assembly [1, 7].

Deep investigations into the self-assembly processes need to consider the influence of both thermodynamic and kinetic factors.

The formation of self-assembled collagen nanofibrils related to the synergistic effect of various intra- and intermolecular non-covalent interactions, as hydrogen-bonding, electrostatic, π - π stacking, and Van der Waals interactions. Therefore, the self-assembly process is mainly driven by thermodynamics [8]. The interference of kinetic parameters such as temperature, pH, and ionic strength can affect the thermodynamic interactions. However, for the time being, knowledge on the thermodynamic and kinetic properties of collagen self-assembly is still in its infancy.

Due to health problems caused by mammalian collagen and religious barriers, other collagen sources are being considered. Therefore, fish wastes are considered as alternatives to collagen sources [9]. There are many studies about the extraction of type I collagen from fish scales [9–12]. Type I collagen possesses a highly repetitive amino acid sequence [Gly-X-Y]_n, where X and Y are proline and hydroxyproline, respectively [10, 13].

Collagen derived from marine species living in warmer environments than those living in cooler environments present higher thermal stability and a higher melting point because they have higher contents of proline and hydroxyproline [14, 15]. In the present study, ASC from the Caspian white fish (*Rutilus Frisiikutum*) scales, was isolated and characterized. Also, the effects of temperature, concentration, pH, and ionic strength on the kinetics and thermodynamic formation of ASC fibrils were investigated. This aim of the present study was to provide a direction for controlling the kinetics/thermodynamic parameters of ASC self-assembly. This may lead to the development of functionalized ASC assemblies.

Materials and Methods

Materials

The Caspian white fish (*Rutilus Frisiikutum*) scales were collected from fish markets and transferred to the laboratory in ice. To remove the debris, the scales were washed with cold distilled water. All the used reagents were of analytical grade.

Collagen Extraction

At first, the fish scales were demineralized. Briefly, the fish scales were washed in 20 mM EDTA, 1 M NaCl, and 50 mM Tris-HCl solution at pH = 7.5 for 48 h, to remove unnecessary proteins on the surface through stirring the solution two days. Demineralization was done by the treating with 0.5 M EDTA (1:10 w/v) at pH = 7.5 for next two days. Then, the scales were washed with distilled water [9]. The demineralized fish scales were chopped into smaller pieces and extracted with 0.5 M acetic acid at pH = 2.5 for 3 days at 4 °C. They were then centrifuged at 3000 g for 15 min, and the supernatants were collected. Salting-out was carried out through adding NaCl to the final concentration of 0.9 M and retained undisturbed for 24 h at 4 °C. The suspension was centrifuged at 8000 g for 1 h, and the pellet was resolubilized in 0.5 M acetic acid. The extracted collagen was dialyzed applying a dialysis membrane (cut-off range – 3 kDa) toward 0.1 M acetic acid and then lyophilized [9].

The Characterization of the Extracted Collagen

TGA

The TGA was used to analyze the demineralized fish scale to approve the whole dissolution of calcium phosphate. The TGA of demineralized scales was undertaken from 0 °C to 620 °C using TGA instrument (TA Instruments, STA 504 model, New Castle, USA).

SDS-PAGE

SDS-PAGE electrophoresis was performed on 7.5% separating gel and 4% stacking gel via Laemmli method [16]. The electrophoresis was done at 100 V, in constant voltage. The gels were stained by Coomassie Brilliant Blue R250.

FT-IR Spectroscopy

The lyophilized collagen was combined with about 50 times of vacuum dried KBr and pressed into a disk using a hydraulic press. The infrared spectra were recorded using a fourier

transform IR spectrophotometer (Bruker Tensor 27) in the range of 4000 to 400 cm^{-1} with an automatic signal gain collected at the resolution of 4 cm^{-1} .

Denaturation Temperature of ASC

The collagen denaturation temperature was analyzed through differential scanning calorimetry (DSC, NETZSCH, F01-DSC) [15]. The extracted collagen was dissolved in 0.1 M acetic acid at 1:40 (*w/v*). After 2 days at 4 °C, the samples were carefully sealed into aluminum pans and were scanned over -20 to 100 °C, with a heating rate of 1 °C/min. N_2 liquid was used for cooling, and an empty sealed pan was used as the reference. According to Kittiphattanabawon et al. [15], the denaturation temperature and enthalpy change were evaluated through the peak of the DSC transition curve.

FE-SEM Images

The surface morphology analysis of the collagen fibrils was examined with a field emission scanning electron microscope, (FE-SEM MIRA3-XMU, TESCAN). Briefly, the collagen was transferred to the aluminum stubs. The collagen molecules were ion-sputtered to minimize charging with a thin gold coating at 2–3 nm thickness using a single gun, argon ion beam sputterer (EMITECH k450x) operated at 5×10^{-3} Pa pressure, 10–20 mA current, and 4 min coating time, using a 15 kV accelerating voltage.

The Self-Assembly of ASC

The ASC fibrillogenesis was assessed by turbidity measurements [17]. 10X phosphate buffered saline (PBS) and 0.1 N NaOH were used in the following experiments. The collagen fibrillogenesis was observed at different times at the absorbance of the solution at 400 nm using a UV-Vis spectrophotometer (PG Instruments Ltd. T80-UV/Vis). The end of the experiment was the time when there was no change in turbidity. The turbidity-time curve was used to study the kinetic self-assembly of collagen. Each experiment was repeated twice.

The Effect of Concentration

The fibrillogenesis of collagen was done in different concentrations of collagen from 0.125 mg/ml to 2.5 mg/ml. For each concentration, the ASC was dissolved in 0.012 M HCl by stirring at 4 °C and then it was mixed with 10X PBS and 0.1 N NaOH (8:1:1) to provide the composition of 10 mM PBS and 168 mM of NaCl.

The Effect of Temperature

The fibrillogenesis of collagen solution at different temperatures was carried out from 12 °C to 20 °C. The ASC solution (ultimate concentration 0.25 mg/mL) was prepared in the same manner as the above-mentioned condition (8:1:1).

The Effect of pH and Ionic Strength

The ASC (ultimate concentration 0.25 mg/ml) was prepared with 10X PBS and 0.1 N NaOH (8:1:1). Different pH values (3.82, 4.38, 5.28, 6.76, 7.26, 8.68, and 9.32) were adjusted by 1 M NaOH or 1 M HCl. The ionic strength effect was investigated at different NaCl concentrations (9.5–3.04 mg/ml) at 14 °C.

Results

TGA Analysis

The demineralization of fish scales was completed after 48 h of EDTA treatment, and was confirmed by TGA-DTA analysis. Figure 1 displays no major weight loss before 100 °C. The weight loss occurred during 100–120 °C, which was the water loss of crystallization. A major weight loss happened between peaks 220 and 450 °C, which could be attributed to collagen decomposition. The last weight loss occurred during 450–600 °C, which was due to the combustion of organic components [18].

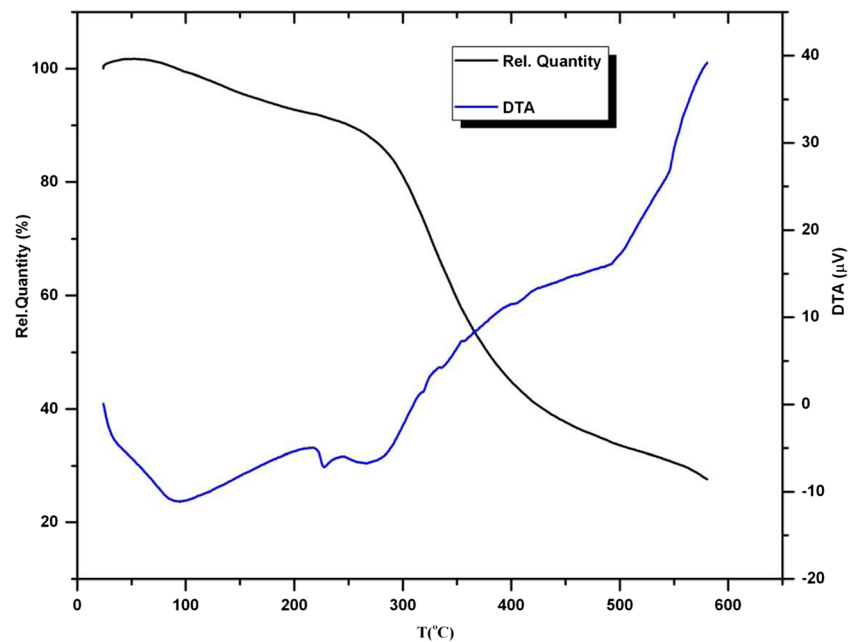
SDS-PAGE Electrophoresis Analysis

The extracted collagen was examined by SDS-PAGE (Fig. 2). Subunit compositions contain two different α chains, $\alpha 1$ and $\alpha 2$, with molecular weights estimated between 110 and 140 kDa, and the intensity of $\alpha 1$, higher than $\alpha 2$. The β chain observed on SDS-PAGE with molecular weight was estimated to be less than 250 kDa, which was the result of cross-linking between the α chains and collagen denaturation during sample preparation for electrophoretic separation. The electrophoretic pattern and the mobility of collagen suggested that the ASC was similar to type I collagen [9, 14, 19]. ASC yields were approximately 1.21% (based on a dry weight).

DSC Analysis

The thermal stability of proteins is indicated by the denaturation temperature. The T_d of ASC and the endothermic heat flow were determined by DSC. Thus, the T_d of the Caspian white fish scale collagen was about 19 °C (Fig. S3). The T_d of

Fig. 1 TGA-DTA curve (% quantity) of demineralized fish scale after 48 h of EDTA treatment



collagen was also reported for Alaska pollack (16.8 °C) [6], and the Antarctic Ice-fish (15 °C). The T_d of collagens was influenced by imino acid contents (proline and hydroxyproline), body temperature, and environmental temperature [13, 15, 20].

The enthalpy of collagen denaturation (ΔH) was determined to be 9.6 J/g (Fig. 3). The ΔH of collagen from differ-

ent species was also different due to the specific sequences of amino acids and their impact on the stability of the triple helix [10]. Also, other factors such as hydrogen bonds in the inner coil-coiled chains and the Gly-Pro-Hyp tripeptide sequence may affect the stability of collagen.

FT-IR Spectroscopy

The FT-IR spectra of ASC from the Caspian white fish scale are depicted in Fig. 4. As it is shown, the amide A absorption band is located at 3428 cm^{-1} , which is associated with N-H stretching coupled with hydrogen bonding [21]. Also, the amide B band positions were found at 2924 cm^{-1} , which were related to an asymmetrical stretch of CH_2 [22]. The amide I band in 1649 cm^{-1} is associated with carbonyl group vibrations, which is coupled with N-H bending vibrations. This indicates the formation of hydrogen bonds between N-H groups and C = O groups, CN stretch and CCN deformation to the formation of the triple helix [23].

The amide II absorption can originate from the wave number of 1553 cm^{-1} , which is mostly related to the combination of CN stretching, and the NH vibration of in-plane bending [24]. The peaks of amide I and amide II of ASC of Caspian white fish scale (1649 cm^{-1} and 1553 cm^{-1} , respectively) were at higher frequencies than those of ASC of Catla (1643 cm^{-1} and 1558 cm^{-1} , respectively) [9], and pepsin-solubilized collagen (PSC) from the skin of black carp (1633 cm^{-1} and 1548 cm^{-1} , respectively) [25]. The shift of these peaks to higher frequencies was related to an increase in the molecular order [23]. The amide III band in 1235 cm^{-1} is a complex band, consisting of components from C-N stretching

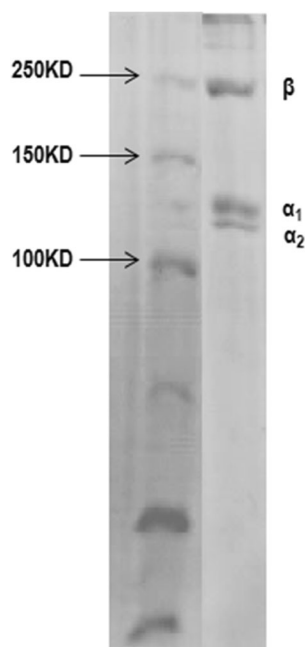
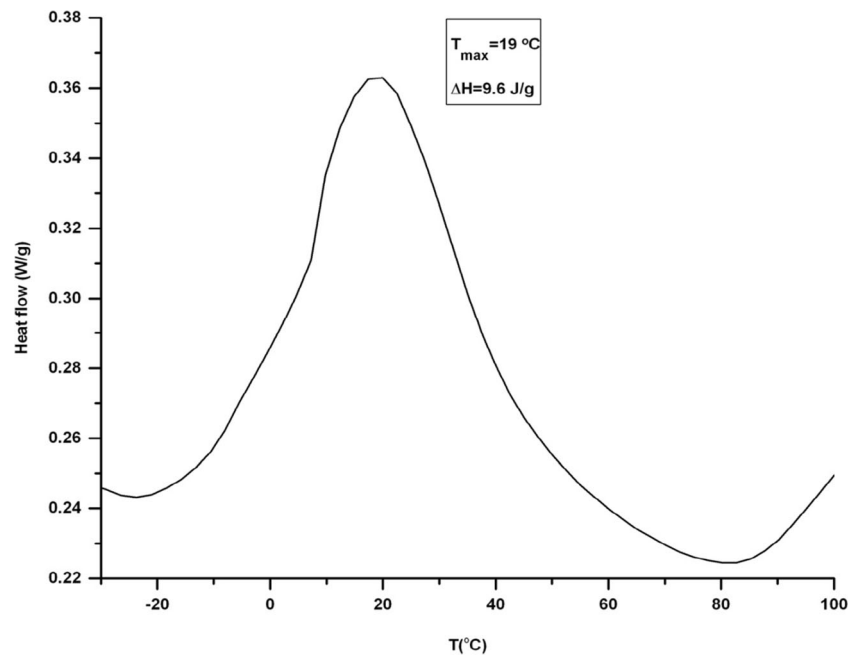


Fig. 2 The SDS-PAGE pattern of ASC from the Caspian white fish scale on 12.5% acrylamide gel. Lane 1 shows protein marker and the other shows ASC

Fig. 3 The DSC thermogram of ASC from the fish scale



and N-H in-plane bending from amide linkage. It is also formed by the absorptions of wagging vibrations from CH₂ groups from glycine backbone and proline side-chains [23]. The results are in accordance with Pati [9], Duan [24], and Muyonga [22].

FE-SEM Images

The FE-SEM was provided with a high resolution (nm scale) to investigate the fibril characteristics and the morphology of collagen. The FE-SEM micrographs of nano-fibril collagen have indicated that the diameter of collagen fibers has varied from 38.3 to 71.5 nm. As seen in Fig. 5, the collagen has a regular lattice, uniform, and has a porous

structure. The porous structure of the collagen was shown later [26].

The Kinetic and Thermodynamic Studies of Self-Assembly of ASC

The kinetic self-assembly of ASC can be assumed by the absorbance changes of the solution at 400 nm. The assembly can follow the first-order rate law [7]. Then, it can be calculated using eq. (1):

$$kt = -\ln \frac{A_e - A_t}{A_e - A_0} \quad (1)$$

Fig. 4 The FT-IR spectrum of the fish scale collagen

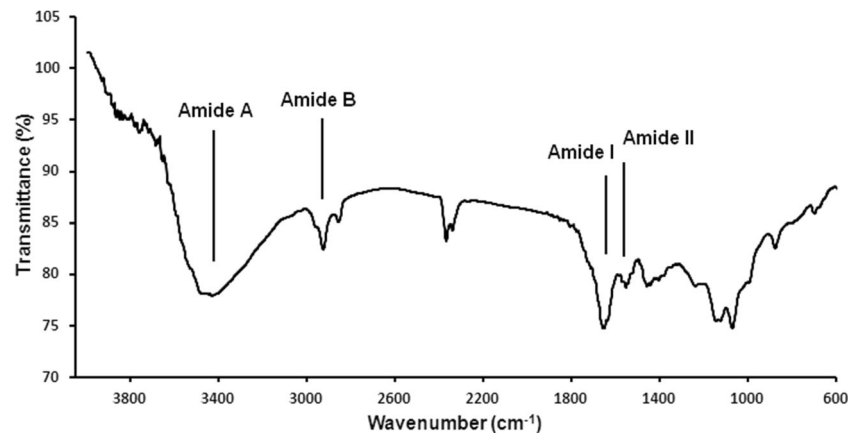
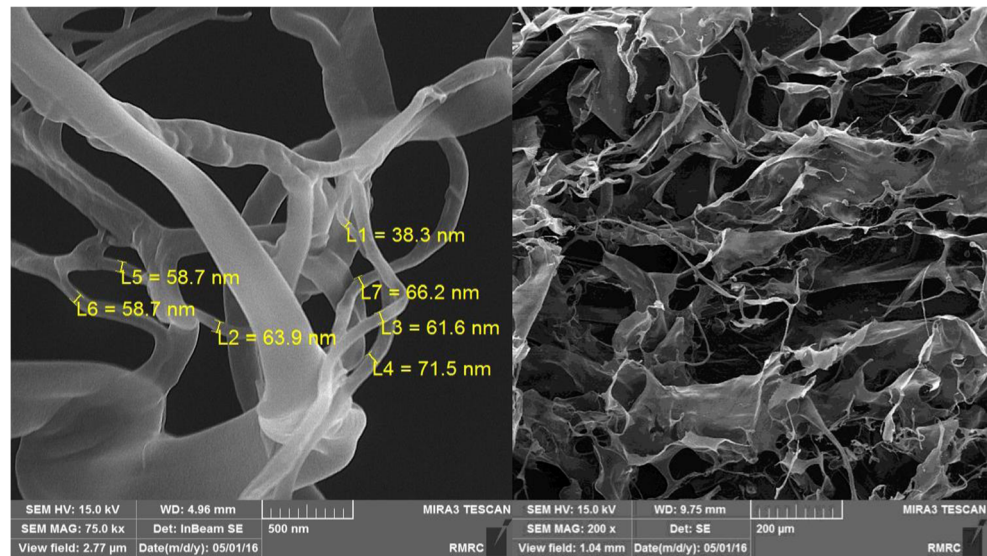


Fig. 5 The FE-SEM images of the Caspian white fish scale collagen



where k is the rate constant calculated from the slope plotting $\ln A_c - A_t / A_c - A_0$ versus time (t); A_0 is the absorbance at 400 nm at time $t = 0$; and A_c is the absorbance at 400 nm at the equilibrium state; A_t is the absorbance at 400 nm at time t . The half-time, which is the time the turbidity reaches half of the finally attained value at a given physiological condition is calculated based on the following equation:

$$t_{1/2} = \frac{0.693}{k} \quad (2)$$

It is assumed that the aggregation of the collagen involved an activation step. The rate of self-assembly at the surface of a fibril was controlled by the activation energy. In principle, the kinetic of self-assembly may be controlled by both an activation step and by the final strength of the intermolecular interactions [27]. The Arrhenius equation is used to calculate the activation energy, E_a (kJ/mol), for fibril formation:

$$k = A e^{-\frac{E_a}{RT}} \quad (3)$$

Where A is the frequency factor (s^{-1}), which depends on the reaction entropy according to the Eyring-Polyanyi equation [28]. E_a is related to the reaction activation enthalpy. A plot of $\ln(k)$ versus T^{-1} gives a straight line whose slope and intercept can be used to define E_a and A , respectively. With employing the transition state theory, the Eyring equation was suggested to describe the relationship for the temperature dependence of a rate constant in a form which is mathematically similar to the Arrhenius equation:

$$k = \frac{k_B T}{h} \exp(-\Delta G^\ddagger / RT) \quad (4)$$

Where k_B is Boltzmann's constant, h is Planck's constant, and ΔG^\ddagger is the Gibbs free energy of activation.

$$\ln \frac{k}{T} = -\frac{\Delta H^\ddagger}{R} \frac{1}{T} + \ln \frac{k_B}{h} + \frac{\Delta S^\ddagger}{R} \quad (5)$$

In the above equation, E_a from eq. 3 could be replaced with ΔH^\ddagger , the activation enthalpy for the reaction, which follows from the Gibbs-Helmholtz relationship for $\Delta G/T$ with respect to $1/T$.

The Effect of Concentration

Concentration is a primary factor influencing the self-assembly of collagen. Collagen turbidity at different concentrations (0.125–2.5 mg/ml) is depicted in Fig. 6-a. The curve contains an initial lag phase with no turbidity change, a growth phase with an increase in turbidity, and a plateau without any further changes in turbidity.

Figure 6a shows that the principal concentration for collagen self-assembly is less than 0.25 mg/ml, below which no turbidity could be detected. It was observed that as the collagen concentration increased, the turbidity rate increased with a sigmoidal curve [29, 30]. It seems that as collagen concentration increases, intra- and inter-molecular hydrogen bonds increase [31]. Therefore, the self-assembly pathway of collagen triple helices is concentration dependent, and the different architectures of fibrillar formation may result from the balance between collagen-collagen and collagen-water molecules via hydrogen bonding interactions.

The plot of $\ln(A_c - A_t / A_c - A_0)$ of ASC versus time at various concentrations is given in Fig. 7. As it can be seen, the breaking point of curves matched with the time in which the absorbance at 400 nm initiated to rise. The same trend was also reported for pollock skin collagen [7], suggesting that the molecular mechanism of collagen self-assembly is a two-phase process. In the first phase, the collagen monomers

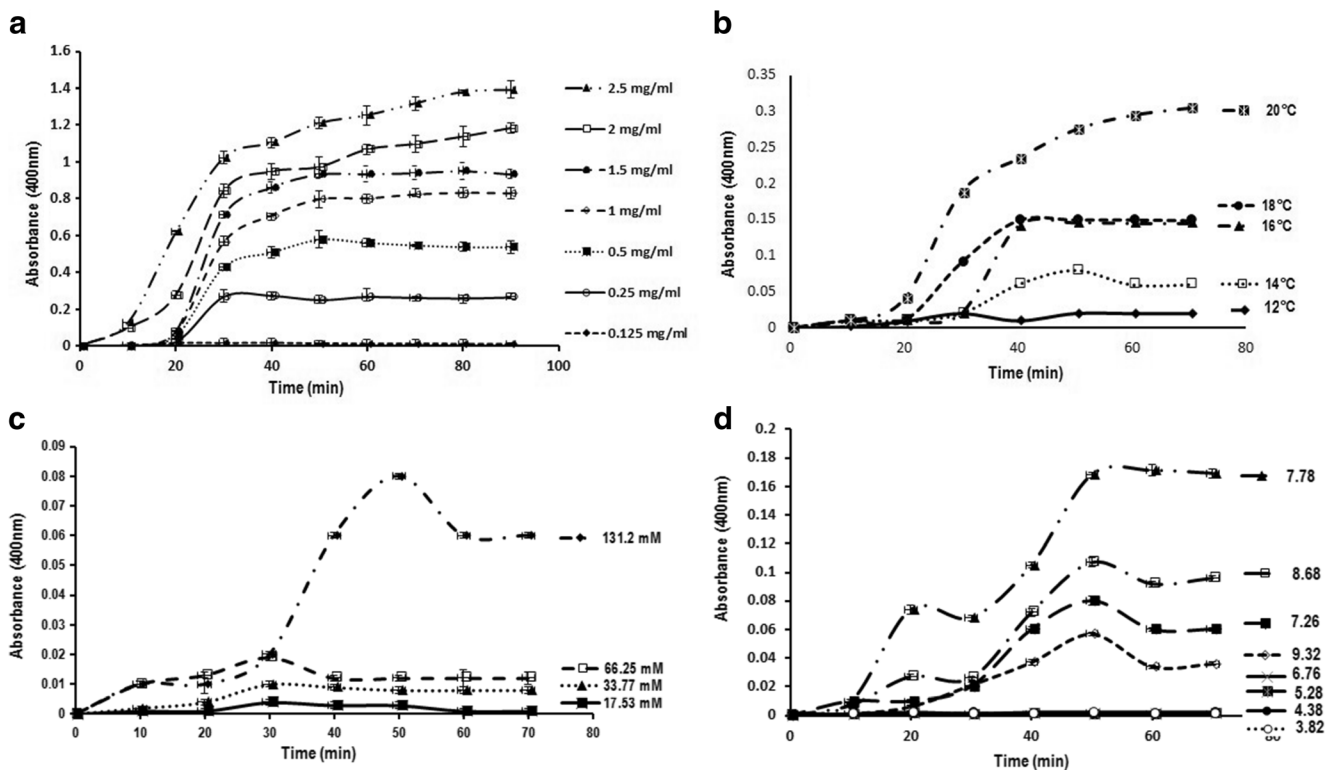


Fig. 6 The effect of concentration (a), temperature (b), ionic strength (c), and pH (d) on the kinetic self-assembly of collagen from the Caspian white fish scale. Note: ASC concentration = 0.25 mg/ml, pH = 7 ± 0.1 and $T = 14$ °C

assemble with each other to form a microfibril, which cause the nucleus center, and then a cooperative nucleation-growth mechanism causes these microfibrils to interact with each other so as to form the collagen fibrils.

The $t_{1/2}$ of the second phase at different collagen concentrations are shown at Table 1. As it can be seen, the self-assembly of ASC takes place at shorter $t_{1/2}$ at higher concentrations. This could be due to the fact that there were more collagen molecules to play the role of nucleation centers during the fibril formation process.

The Effect of Temperature

The effect of temperature on collagen turbidity is illustrated in Fig. 6b. The curves possess an initial lag phase, a growth phase, and a plateau. There is no turbidity below 14 °C. With the increase of temperature, the self-association rate elevates. During the fibril formation process, there are intermolecular interactions such as a Van der Waals attractive, a repulsive electrostatic, and a hydrophobic attractive force. Figure 6b shows that the temperature between 16 °C to 20 °C is suitable for fibril formation. The weak absorption at 12 °C indicated the formation of a small amount of thin fibril. The plot of $\ln(A_e - A_t / A_e - A_0)$ of ASC versus time at various temperature is provided in Fig. S1. The time to initiate the second phase occurs faster with the increase of temperature, showing that the reaction rate

is based on temperature. The findings indicate that collagen fibrils formation and their growth increase as the temperature rises, and the rate constants (k) increase, as well. These results are in accordance with those of others [7, 32]. According to Table 1, a stronger cooperative nucleation-growth mechanism at higher temperature can lead to a shorter $t_{1/2}$. That means that fibrils formation can become mature faster.

The k and the $t_{1/2}$ of the growth phase at different temperatures are depicted in Table 1. The shorter $t_{1/2}$ and faster k at higher temperatures reveal that the cooperative nucleation-growth mechanism self-assembly of collagen is a temperature dependent process. From the Arrhenius plot, Fig. S2-a, $E_a = 44.3$ kJ/mol and $A = 117 \times 10^5$ s $^{-1}$. From Eyring plot, Fig. S2-b, $\Delta H^\ddagger = 42.98$ kJ/mol and $\Delta S^\ddagger = -0.12$ kJ/mol.K.

The negative value of ΔS^\ddagger indicates an intermolecular associative mechanism in which every two or more collagen molecules form an activated complex. The positive values of ΔG^\ddagger indicates that the activated complex formation is a non-spontaneous process and controlling the external triggers such as pH, ionic strength, temperature, and collagen concentration is necessary for this process. As Table 2 shows, the transition step is a non-spontaneous and endothermic process. Above $T_d = 19$ °C, the turbidity curve of the ASC has a shorter lag phase and a longer growth phase. This could mean that the three-dimensional networks of collagen fibrils can be formed faster.

Fig. 7 The plot of $\ln \frac{A_e - A_t}{A_e - A_0}$ vs. t of the Caspian white fish scale collagen at concentrations of 0.25 mg/ml (a), 0.5 mg/ml (b), 1 mg/ml (c), 1.5 mg/ml (d), 2 mg/ml (e), and 2.5 mg/ml (f)

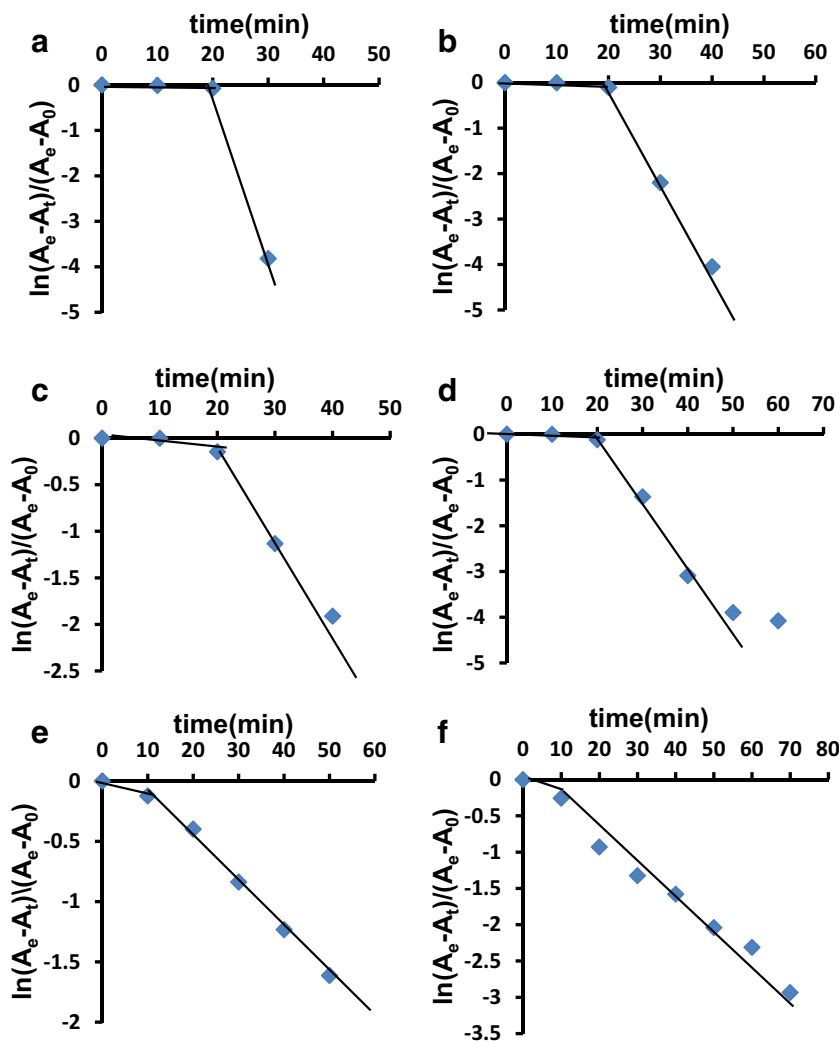


Table 1 $t_{1/2}$ for the growth phase of ASC collagen from the Caspian white fish scale at different physiological conditions

Concentration (mg/ml)	$K \times 10^{-3} \text{ (s}^{-1}\text{)}$	$t_{1/2}(\text{min})$
0.25	215	33.22
0.5	80	28.66
1.0	104	26.66
1.5	123	25.63
2.0	55	22.60
2.5	60	21.43
Temperature (°C)	$K \times 10^{-3} \text{ (s}^{-1}\text{)}$	$t_{1/2}(\text{min})$
14	101	36.86
16	118	35.87
18	133.5	25.19
24	189.5	13.02
26	292.2	12.61

The Effect of Ionic Strength

The solubility of fish scale collagen at different NaCl concentrations is depicted in Fig. 6c. The collagen solubility is often reduced with an increase in NaCl concentration [7, 15]. The results indicate that the turbidity increases significantly in 131.2 mM salt concentration. This phenomenon could be associated with the reduction of repulsion between collagen molecules [2]. At lower

Table 2 The thermodynamic parameters of ASC from the Caspian white fish scale at transition state

Temperature(°C)	$\Delta G^\ddagger(\text{kJmol}^{-1})$	$\Delta H^\ddagger(\text{kJmol}^{-1})$	$\Delta S^\ddagger(\text{kJmol}^{-1} \text{ K}^{-1})$
14	75.76	42.08	-0.12
16	75.85		
18	76.23		
24	77.00		
26	77.00		
30	77.60		

concentrations, the weakening in cooperative nucleation-growth mechanism is due to Debye-Hückel screening effect, and suggests the formation of ion pairs in the association.

The Effect of pH

Electrostatic interaction is crucial in the formation of collagen fibrils. In the current study, the electrostatic interactions were controlled by changing the pH. Figure 6d illustrates the influence of pH on self-assembly of the ASC. The absorbance in 400 nm showed that the fish scale collagen was self-assembled in the range of pH = 7.26 to 9.32. It was indicated that in pH ranges less than 7.26, the repulsion between the collagen molecules were higher than the attraction between them, causing high solubility in the acidic range. By increasing the pH to 9.32, the repulsion between the collagen molecules decreased, causing the self-assembly of collagen. This is in line with studies in which the highest solubility was observed at pH < 7 [7, 15, 33]. The plot of maximum absorbance of collagen from the fish scale versus different pH values is given in Fig. 3S. It seems that the Isoelectric point (pI) of ASC is about 7.76.

Conclusion

ASC were successfully isolated from the scales of the Caspian white fish. The extracted collagens were identified as type I collagen. The thermal stability of the isolated collagen was relatively low $T_d = 19$ °C, revealing low content of proline and hydroxyl proline, which can be applied for gelatin extraction. There are apparent effects of concentration, pH, temperature, and ionic strength on ASC kinetics of self-assembly. The self-assembly is followed by two-phases, a lag phase, and a growth phase. The optimum condition for the self-assembly is determined at pH = 7., $T = 14$ °C, NaCl concentration = 131.2 mM, and collagen concentration = 0.25 mg/ml. The negative value of ΔS^\ddagger , and the positive value of ΔG^\ddagger reveal that the activated complex formation is a non-spontaneous endothermic process with an intermolecular associative mechanism. Kinetic factors can not only influence the self-assembly structure of ASC but also regulate the activation complex structure in the transition state. With the precise control of the self-assembly of ASC, multifunctional architecture can be created. This may encourage the development of ASC from the Caspian white fish scale towards drug delivery and tissue engineering applications.

Acknowledgements This work was supported by the Department of Marine Chemistry, Faculty of Marine & Oceanic Sciences, University of Mazandaran, Babolsar, Iran.

Compliance with Ethical Standards

Conflict of Interest There is no conflict of interests.

References

1. T. Nikolaeva, E. Tiktopulo, R. Polozov, Y.A. Rochev, *Biophysics* **52**(2), 191–195 (2007)
2. K.E. Kadler, A. Hill, E.G. Canty-Laird, *Curr. Opin. Cell Biol.* **20**(5), 495–501 (2008)
3. A.O. Brightman, B. Rajwa, J. Sturgis, M. McCallister, J. Robinson, S. Voytik-Harbin, *Biopolymers* **54**(3), 222–234 (2000)
4. Y.-I. Yang, L.J. Kaufman, *Biophys. J.* **96**(4), 1566–1585 (2009)
5. G. Forgacs, S.A. Newman, B. Hinner, C.W. Maier, E. Sackmann, *Biophys. J.* **84**(2), 1272–1280 (2003)
6. S. Kimura, Y. Ohno, *Comp. Biochem. Physiol. B: Comp. Biochem.* **88**(2), 409–413 (1987)
7. M. Yan, B. Li, X. Zhao, S. Qin, *Food Hydrocoll.* **29**(1), 199–204 (2012)
8. J.J. McManus, P. Charbonneau, E. Zaccarelli, N. Asherie, *Curr. Opin. Colloid Interface Sci.* **22**, 73–79 (2016)
9. F. Pati, B. Adhikari, S. Dhara, *Bioresour. Technol.* **101**(10), 3737–3742 (2010)
10. T. Ikoma, H. Kobayashi, J. Tanaka, D. Walsh, S. Mann, *Int. J. Biol. Macromol.* **32**(3), 199–204 (2003)
11. Y. Nomura, H. Sakai, Y. Ishii, K. Shirai, *Biosci. Biotechnol. Biochem.* **60**(12), 2092–2094 (1996)
12. Y. Zhang, W. Liu, G. Li, B. Shi, Y. Miao, X. Wu, *Food Chem.* **103**(3), 906–912 (2007)
13. A.V. Persikov, J.A. Ramshaw, A. Kirkpatrick, B. Brodsky, *Biochemistry* **39**(48), 14960–14967 (2000)
14. T. Nagai, N. Suzuki, *Food Chem.* **68**(3), 277–281 (2000)
15. P. Kittiphattanabawon, S. Benjakul, W. Visessanguan, T. Nagai, M. Tanaka, *Food Chem.* **89**(3), 363–372 (2005)
16. U. Laemmli, *Nature* **227**, 680–685 (1970)
17. J.L. Brokaw, C.J. Doillon, R.A. Hahn, D.E. Birk, R.A. Berg, F.H. Silver, *Int. J. Biol. Macromol.* **7**(3), 135–140 (1985)
18. A. Bigi, A. Ripamonti, G. Cojazzi, G. Pizzuto, N. Roveri, M.H.J. Koch, *Int. J. Biol. Macromol.* **13**, 110–114 (1991)
19. F. Zhang, A. Wang, Z. Li, S. He, L. Shao, *Food Nutr. Sci.* **2**(8), 818 (2011)
20. T. Nagai, N. Suzuki, T. Nagashima, *Food Chem.* **111**(2), 296–301 (2008)
21. K.P. Sai, M. Babu, *Comp. Biochem. Physiol. B: Biochem. Mol. Biol.* **128**(1), 81–90 (2001)
22. J.H. Muyonga, C.G.B. Cole, K.G. Duodu, *Food Chem.* **86**(3), 325–332 (2004)
23. K. Payne, A. Veis, *Biopolymers* **27**(11), 1749–1760 (1988)
24. R. Duan, J. Zhang, X. Du, X. Yao, K. Konno, *Food Chem.* **112**(3), 702–706 (2009)
25. G.P. Wu, X.M. Wang, L.P. Lin, S.H. Chen, Q.Q. Wu, *Adv. Biosci. Biotechnol.* **5**, 642–650 (2014)
26. T. Ikoma, H. Kobayashi, J. Tanaka, D. Walsh, S. Mann, *J. Struct. Biol.* **142**(3), 327–333 (2003)
27. A. Cooper, *Biochem. J.* **118**(3), 355–365 (1970)
28. H. Eyring, *J. Chem. Phys.* **3**(2), 107–115 (1935)
29. P. Noitup, M.T. Morrissey, W. Garnjanagoonchorn, *J. Food Biochem.* **30**(5), 547–555 (2006)
30. N. Aukkanit, W. Garnjanagoonchorn, *J. Sci. Food Agric.* **90**(15), 2627–2632 (2010)
31. R. Usha, T. Ramasami, *Thermochim. Acta* **409**(2), 201–206 (2004)
32. D.L. Christiansen, E.K. Huang, F.H. Silver, *Matrix Biol.* **19**(5), 409–420 (2000)
33. P. Singh, S. Benjakul, S. Maqsood, H. Kishimura, *Food Chem.* **124**(1), 97–105 (2011)